HIFI Stability
as Measured During ILT Phase

J. W. Kooi [1*], V. Ossenkopf [2, 4], M. Olberg [3, 4], R. Shipman [5],

R. Schieder [2], and D. Teyssier [6]

[1]*California Institute of Technology, Pasadena, CA 91125, USA*

[2]*KOSMA, I.Physikalisches Institut der Universitat zu Köln, Germany*

[3]*Onsala Space Observatory, Sweden*

[4]*SRON Netherlands Institute for Space Research, Groningen, the Netherlands*

[5]*University of Groningen, Kapteyn Astronomical Institute, Groningen, the Netherlands*

[6] *European Space Agency Centre (ESAC), Spain*

* Contact: kooi@caltech.edu, 626-395-4286

Abstract— **We present here the stability results of the high frequency heterodyne instrument (HIFI), to be flown on the Herschel space observatory. The measurements were taken as part of the instrument level tests (ILT) in the spring of 2007. Herschel is ESA's fourth cornerstone mission in the Horizon 2000+ program, and aims at observations in the Far-InfraRed and sub-millimeter wavelength region. HIFI itself is one of three instruments onboard Herschel. The other two being PACS, the photodetector array camera and spectrometer, and SPIRE, the spectral and photometric imaging receiver.**

The detailed instrument stability measurements were conducted to establish the functionality, and observational readiness of the instrument.

I WHY TO MEASURE (HIFI) INSTRUMENT STABILITY

HIFI is a probably the most complex and sensitive heterodyne instrument ever put together. It consists of 7 mixer bands covering the frequency range from 480 GHz to 2 THz. Mixer bands 1-5 are based on Superconductor-Insulator-Superconductor (SIS) technology whereas bands 6-7 are Hot-Electron Bolometer (HEB) based. Each mixer band consists of two mixers, sensitive to either horizontal or vertical polarization (14 mixers in all). These, along with the diplexers and beam splitters are housed in the Focal Plane Unit, or FPU (Fig. 1). To provide the mixers with a local oscillator signal, 14 multiplier chains (driven by power amplifiers) are contained in a separate Local Oscillator Unit (LOU). The LOU is driven by a custom designed Local oscillator Source Unit (LSU). The LCU, shown in Fig. 1 provides the required bias voltages and interfaces to the common instrument bus. The mixer output signals are after (cold) amplification routed to two 4 GHz wide Acousto-optical spectrometer's [1, 2], and two 2 GHz wide auto-correlation spectrometers [3] (one for each polarization). The wideband acousto-optical spectrometer's (WBS) consist of four 1 GHz wide subbands, 2000 channels each. Thus the 'full' spectrometer has 8000 spectral channels. The digital correlator, or high resolution spectrometer (HRS) has a total processing bandwidth of 2 GHz, and consists of 8 channels or subbands. The HRS can be programmed for different frequency resolutions anywhere within the mixer IF passband. Essentially all stability measurements were performed with both WBS and HRS. The derived Allan variance stability measurements for both types of spectrometers is basically the same, provided the difference in noise fluctuation bandwidth is taken into account. The HRS is found to be quite a bit less sensitive to thermal drift then the WBS, which should not come as a surprise.

As is evident from Fig 1, there are ample opportunities for degrading effects from thermal, electronic drift, gain fluctuations, optical and IF standing waves, mechanical vibrations, ground loops, and electromagnetic interference.

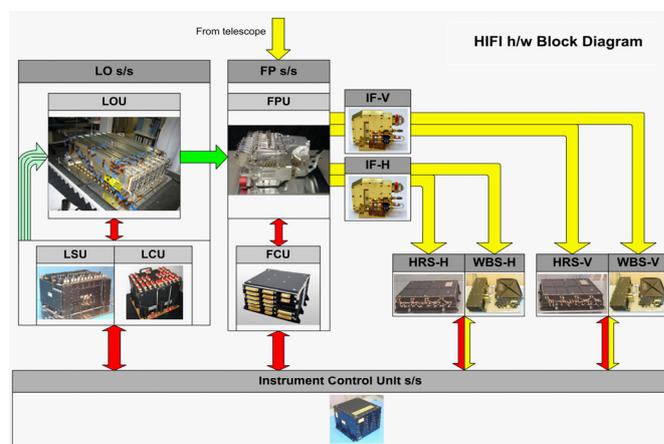We list here the primary reasons for studying the stability of the instrument. They are:

Fig. 1. Block diagram of HIFI. The different units are discussed in the text.

A. Optimize astronomical observing modes.
B. Study 14 mixer/LO sub-bands and identify problem area's.
C. Determine the observation efficiency loss due to instability (Compute the rms noise level).
D. Search for platforming effects, baseline ripple, offsets…

The obtained stability data (Allan time, drift slope, Section III) is fed into the Herschel Observation Planning Tool (HSPOT), and Astronomical Observation Techniques (AOT's). In Fig. 1 we show the block diagram of HIFI[4], the heterodyne instrument for ESA's **Herschel** space satellite[5].

II WHAT DO WE MEASURE

There are many facets to establishing the stability performance of the instrument. Listed categorically they are:

A. IF stability
B. Time Constants
   - IF amplifier warm-up
   - LO warm-up
   - Spectrometer warm-up
C. System stability for each mixer in 14 LO sub-bands
   - Total power amplitude stability
   - Spectroscopic stability
D. Differential gain stability
   - Dual beam switching (DBS)
   - Load Chop (LS)
   - Internal Load
   - Frequency switching (FSW)
E. Parametric Stability
   - B-field at the SIS bands
   - Stability as a function of LO power
   - Stability as a function of bias voltage

The instrument IF stability is measured without LO signal and with the SIS and HEB mixers biased at 8 mV. IF stability establishes the performance of the joint IF and backend signal chain.

Warm up time constants are important in establishing boundary conditions for instrument operation. HIFI will be on approximately 1/3 of the mission life time, it sharing time with PACS and SPIRE. Thus it is important to know how long the IF amplifiers, local oscillators, and spectrometers have to be turned on before certain types of observations may commence.

System stability establishes the total power and spectroscopic stability of the instrument. These are needed to determine switch rates (section VIII), mapping strategies, and to give a measure of how often to calibrate for absolute flux observations. In an ideal instrument, position switching (slewing the entire telescope off source for a reference measurement) is the most efficient observation mode. Often however the spectroscopic stability time is such that position switching is not possible (too slow). In this case relatively fast differential 'on-off' source measurements performed.

The differential stability tests thus measures the efficiency and baseline quality of a number of switched observing modes.

Symmetric dual beam switching (on-off-off-on...) on HIFI can occur at a maximum rate of 0.25 Hz, or 4 s. This is the time required to readout all four spectrometer channels, and is known as 'slow-chop'. It is also possible to switch as fast as 4 Hz, in an 'on-off-on-off...' pattern. It this case a 25 % penalty is paid by buffering the spectrometer data in the internal spectrometer buffers. Thus for the sake of time efficiency slow-chop is preferred. DBS is accomplished by nutating an internal FPU mirror. Only small beam throws (180'') are possible. This mode is only effective therefore for compact sources. For extended line sources Load-Chop (LS) may be used. LS switches periodically against an internal load. On the ground this technique cannot be easily applied due to the interfering effect of the atmosphere. As we shall see, both DBS and LS loose a factor of 4 in integration time (2 in noise) over an ideal position switching instrument

Internal Load measures a reference beam on two internal calibration loads. In doing so it established the secondary calibration loop time. We find values of $>= 20$ minutes for the SIS bands, and 15 minutes for the HEB mixer bands.

Frequency switching is a promising, but not fully demonstrated mode. In this case the LO source frequency is modulated by a small amount. This will allow observations of the source in both the 'on' and 'off' position, thereby doubling the integration efficiency over DBS and LS. The object is to keep the LO pump level on the mixer constant. Thus it is very important to establish the dominant optical standing wave in the system. Dedicated in flight tests are setup to determine the primary standing waves within the telescope.

Finally we have parametric stability. Since telemetry to the instrument is only once a day, the mixers and local oscillators will have to be run autonomously. Thus it is important to establish bias ranges over which the instrument can be expected to perform as expected.

III HOW DO WE MEASURE STABILITY

Radio astronomy receivers in general look at very weak signals deeply embedded in noise. To extract the weak signals, synchronous detection (signal on - signal off) is typically employed. This is done by either slewing the whole telescope back and forth so as to get the beam on/off the source, or by moving the secondary mirror (sub-reflector) of the telescope at a certain rate. The problem in both these cases is the dead time between observations, i.e., chopping efficiency (η_c). A practical lower limit for slewing an entire telescope off-source is typically 15 seconds, while chopping the secondary mirror can perhaps be as fast as 0.2 seconds (5 Hz). As we have seen, frequency switching with the HIFI instrument is possible and can be accomplished at a much higher rate. It suffers however from modulation of the LO-Mixer standing wave [6], LO power stability, and for terrestrial observations changes in the atmospheric transmission.

If the noise in the receiver system is completely uncorrelated (white), it turns out that the rate of chopping (modulation frequency) has no effect on the final signal to noise ratio. This can be deduced from the well known radiometer equation which states that the noise integrates down with the square root of integration time

$$\sigma(T) = \frac{2\langle s(t)\rangle}{\sqrt{\eta_c \Delta\nu T}}$$

(1)

Here σ is the standard deviation (rms voltage) of the signal, $\langle x(t)\rangle$ the signal mean, $\Delta\nu$ the effective fluctuation bandwidth, and T is the total integration time of the data set. The factor 2 comes in from the loss of integration time ($\sqrt{2}$), and a factor of $\sqrt{2}$ because of the subtraction of two essentially white (Gaussian) noise signals. η_c is the chopping efficiency (~ 0.95).

In practice, the noise in radiometers, and in particular SIS and HEB mixers, appears to be a combination of low frequency drift (correlated noise), 1/f electronic noise and white (uncorrelated) noise. Hence, there is an optimum integration time, known as the Allan stability time (T_A), after which observing efficiency is lost. In actual synchronous detection measurements ``n'' samples of difference data (signal on - signal off) are taken, each with a period T. These differences are then averaged so that the total observed time equals n*(2T). If the period T is larger than the Allan stability time (T_A) of the system, then apart from loss in integration efficiency, there will be a problem with proper baseline subtraction and intensity calibration. This manifests itself in baseline distortion at the output of the spectrometer (Fig. 2) which severely limits how well the noise integrates down with time Section VIII.

The Allan variance theory has been outlined in [7-10], and we merely present here the conclusions, least to say that the Allan variance is σ_A^2 is historically [11] defined as $\sigma^2/2$. For a noise spectrum that contains drift, white noise, and 1/f noise it is found that the Allan variance takes the form

$$\sigma_A^2(T) = aT^\beta + \frac{b}{T} + c$$

(2)

where *a, b,* and *c* are appropriate constants. For short integration times, the variance decreases as $1/T$, as expected from the radiometer equation. For longer integration times, the drift will dominate as shown by the term aT^β. In that case, the variance starts to increase with a slope β which is experimentally found to be between 1 and 2. For SIS and HEB mixers it is frequently observed that the variance plateaus at some constant level. This is attributed to the constant c and is representative of flicker or 1/f noise in the device under test.

Plotting σ_A^2 vs. the integration time T on a log-log plot demonstrates the usefulness of this approach in analyzing the radiometer noise statistics (Fig. 2). As a reference it is meaningful to superimpose radiometric noise with a T^{-1} slope. The latter represents the uncorrelated (white) noise part

of the spectrum. The minima in the plot gives the Allan time T_A, the crossover of white noise to 1/f or drift noise. Often however, such as in Fig. 2, there is no clear minima and a factor $\sqrt{2}$ deviation from the rms radiometric noise is then a useful definition of the Allan time.

Finally, it is often of interest to estimate what happens to the Allan stability time if spectrometer channels are binned to reduce the rms noise in an observed spectrum, or if the IF bandwidth of the radiometer is increased (different velocity resolution). In this case it can be shown that

$$T_A'/T_A = (\Delta\nu/\Delta\nu')^{\frac{1}{\beta+1}} \ .$$

(3)

β is the slope of the drift noise as discussed above. And T'_A the newly obtained Allan time for fluctuation bandwidth $\Delta\nu'$.

A. Total Power Stability

As an example we show in Fig. 2 the total power, or continuum, Allan variance of HIFI HEB mixer band 6a (H-polarization), as measured during the instrument level test phase (ILT) in May 2007. As we shall see, this plot contains a wealth of information.

The IF output frequency of the HEB mixer is 2.4-4.8 GHz [12], which after being up-converted, and then back down-converted to match the wideband acousto-optical spectrometer [1] input, translates to a WBS subband1 of 4.8-3.8 GHz, a subband2 of 3.8-2.8 GHz, and a subband3 of 2.8-2.4 GHz. 'Full' corresponds to a stability averaged over the the total 2.4 GHz available (HEB) IF bandwidth. It should be noted that the HEB mixer is most sensitive in a 2.4-3.4 GHz IF frequency range [12], and as a results it may be expected that WBS subband 3 is the most unstable. This is indeed consistently the case, as shown in Fig. 2.
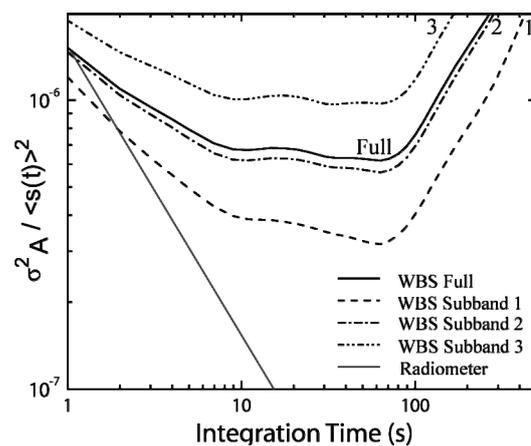

Fig. 2. Normalized total power Allan variance. 'Full' (2.4 GHz) spectrometer response deviates a factor 2 from the radiometric noise at 3 s. This may be considered the effective total power "Allan variance minimum time" (TA). H-polarization, vLO= 1447 GHz. See text for details.

The offsets between the three spectrometer subband Allan times is due to excess noise in each of the IF sub-channels.

Averaged over the entire IF bandwidth, the calculated fluctuation noise bandwidth ($\Delta \nu$) is 1.3 MHz. This is somewhat less then the spectrometer [1] intrinsic noise bandwidth of 2.3~MHz, indicative of excess (non radiometric noise). Again referring to Fig. 2, between 1 and 7 seconds we see the noise integrate down with a slope slightly less then T^{-1}. Judging from the -1 radiometer slope, we have a factor 2 loss in integration efficiency at ~3 s. This may be considered the effective "Allan minimum time". The reason that there is not a clear minimum in the Allan variance plot is that HEB mixers exhibit significant 1/f fluctuation noise (zero slope), as is evident between ~10-90 s. Above approximately 90 s, drift noise begins to dominate. In this particular example the drift slope $\beta = +1.2$.

B. Spectroscopic Stability

The spectroscopic Allan variance measures deviations from the continuum level fluctuations [10]. As such it corresponds to the subtraction of the spectrometer mean continuum level, known as the zero[th] order baseline correction [7, 8, 10]. This is allowed since most heterodyne observations are intended for line observations, rather then continuum or flux calibration. For continuum measurements incoherent detectors are much better suited. Lets assume K spectrometer channels, then the signal in each channel $d_K(n)$ at time n may be normalized by subtraction of the instrument zero level in the particular channel (z_k), and then by dividing the difference by the temporal average of each channel

$$s'_k(n) = \frac{d_k(n) - z_k}{\langle d_k(n) - z_k \rangle_n} , \quad z_k = \frac{1}{N} \sum_{n=1}^{N} d_k(n) .$$

(4)

To now obtain the difference for the spectroscopic Allan variance computation, we subtract the normalized mean summed over all spectrometer channels, e.g.

$$s_k(n) = s'_k(n) - \langle s'_k(n) \rangle_k .$$

(5)

$s_k(n)$ may then be used to obtain the spectroscopic Allan variance for each channel by substitution of $d_k(n)$ with $s_k(n)$ in

$$\sigma^2_{A,k}(T) = \frac{1}{2(N-1)} \sum_{n=1}^{N} (d_k(n) - \langle d_k \rangle)^2 , \quad \langle d_k \rangle = \frac{1}{N} \sum_{n=1}^{N} d_k(n) .$$

(6)

N equals the number of discreet time samples taken. By using Eq. 6 directly ($d_k(n)$ is the temporal data in spectrometer channel k) the total power Allan variance is obtained. To obtain the Allan variance in K spectrometer channels the variance is summed as

$$\sigma^2_A(T) = \frac{1}{K} \sum_{k=1}^{K} \sigma^2_{A,k}(T) .$$

(7)

In Fig. 3 we show the spectroscopic Allan variance. In this case a zero[th] order correlated noise baseline is subtracted. We
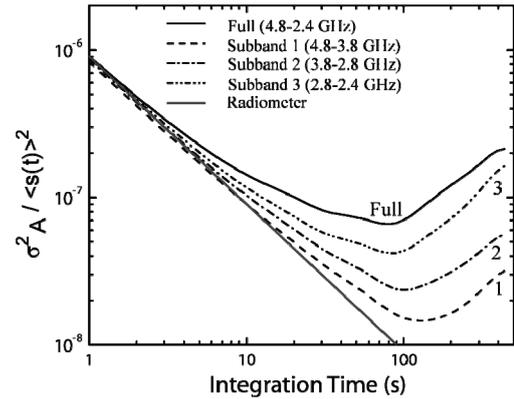

Fig. 3 Spectroscopic Allan variance for the B6a HEB mixer subbands and full spectrometer band (2.4 GHz). The Allan times, defined as a factor of two deviation from the radiometric noise (white) are: TA (full)=14.9 s, TA (subband1)=111 s, TA (subband2)=50.5 s, and TA (subband3)=30.7 s. The noise fluctuation bandwidth is 2.3 MHz. H-polarization, υLO= 1447 GHz.

see a substantial improvement in the statistical variance of the spectra. The noise now integrates down radiometrically, for about 50 s in case of the subbands, and 15 s for the full spectrometer band (4.8-3.8 GHz). The 1/f gain fluctuation noise that dominates the continuum Allan variance of Fig. 2 is now nearly completely removed!

Taking the ratio of the spectroscopic to the total power Allan variance (see Fig. 5), we find that statistically the largest improvement (factor 20+) is gained by spectrometer subband 3 at integration times > 10 s. This is good as most galactic (narrow line) observations will be planned in this subband, being the most sensitive region of the HEB IF passband [12]. For spectral line broadened extragalactic observations the full spectrometer bands needs to be used and a factor of six improvement over the continuum stability is obtained. Continuum measurements will be very challenging.

It should be noted that the HIFI B6a results presented here serve as a typical ILT obtained example of system stability. Actual HEB mixer stability [6] may be better in a more optimized environment such as space, or possibly worse in a poorly designed ground based application.

C. Improvement of Spectroscopic over Total Power Allan Variance.

To compare the improvement in spectroscopic Allan variance over continuum Allan variance, we compare in Fig. 4 the ratios of SIS mixer band 2 (736 GHz), and in Fig. 5 HEB mixer band 6 (1652 GHz). For the HEB mixer, subband 1 has the lowest sensitivity (4.4-4.8 GHz), and also shows the least improvement. The loss in sensitivity of an HEB mixer is caused by the roll off in mixer conversion gain as a function of IF frequency [13], overlaid by the frequency response of the diplexer used to inject the LO signal.

For the band 2 SIS mixer the sensitivity is uniform across all four spectrometer subbands. In this case a beam splitter is used to inject the LO signal. Why the spectroscopic- over
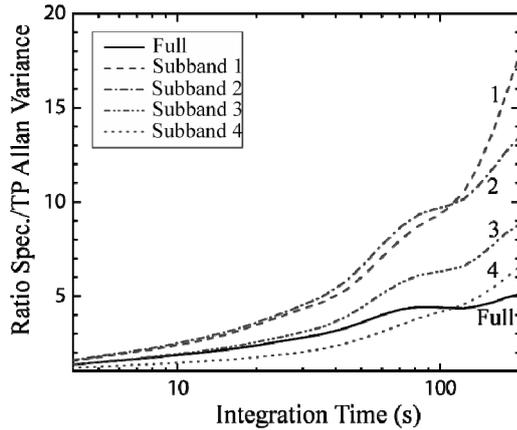
Fig. 4 Improvement ratio of the spectroscopic Allan variance for HIFI SIS mixer band 2b. Shown are the stability results of the four 1GHz wide AOS subbands and the full spectrometer (8000 channels). LO frequency is 736 GHz.

continuum Allan variance ratio is not more uniform is not entirely clear, except to note that the 7-8 GHz IF channel (subband 4) has always the worst stability performance. It is likely that we see an additive effect of the many sub-components in the IF- and backend system. In general it appears therefore that the noise of a SIS mixer is less correlated in the higher end of the IF band (7-8 GHz).

Significantly more spectroscopic- over continuum Allan variance improvement is obtained in the HEB band then the SIS band. There are several explanations for this. First, the HEB is a power sensor. This is opposed to a SIS junction that is sensitive to quasi-particle tunneling through a thin barrier Second, HEB mixers operate in the terahertz frequency regime. As such they are more sensitive to optical standing
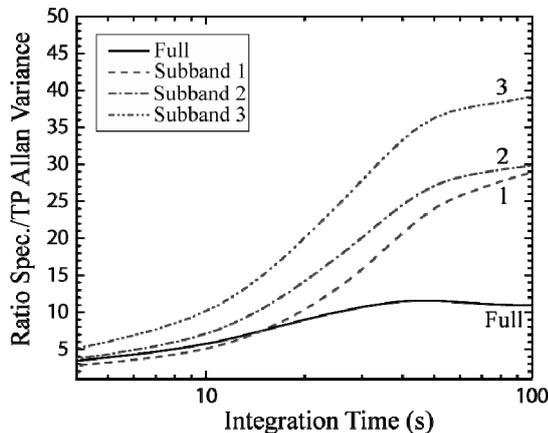

Fig. 5 Improvement ratio of the spectroscopic Allan variance for HIFI HEB mixer band 6b. LO frequency is 1652 GHz. Note that the plots of Fig. 4, 5 have different scales. The removal of a zero[th] order baseline has significantly more effect on a per subband bases for an HEB mixer then SIS mixer. This indicates that the source of HEB instability is highly correlated in an HEB mixer. The most likely culprits are: LO instability and optical standing waves. SIS mixer band 2 is a beamsplitter band, and HEB mixer band 6 uses a diplexer to inject the LO signal. Due to the finite diplexer passband and roll of in mixer gain, HEB subband 1 has considerably lower sensitivity than subband 3. For both mixer bands we have plotted the vertically polarized IF output channel.

waves then SIS mixers, which primarily operate below 1~THz [6]. And finally, the LO sources that pump the mixers are more complex at higher operating frequencies (HEB mixers), and thus more susceptible to amplitude noise which increases approximately as $20\log_{10}(M^2)$ [14]. M is the multiplication factor.

IV SOME EXAMPLE OF WHAT CAN GO WRONG

No system is perfect and neither is HIFI. Here are a few system level examples of what can go wrong: Platforming, high level of gain instability, very short Allan times, and poor subtraction of difference spectra (significant standing waves). These results were part of the initial ILT tests results. The problem was caused by the local oscillator power amplifiers not being driven hard enough into saturation. This resulted in significant amplitude jitter (noise) at the multiplier outputs. The solution was to insert optical attenuators in the LO signal path, so as to force the power amplifiers in a more optimum bias regime. A paper by Jellema *et al,* in this proceedings provides more details on the design, measurement, and material properties of the above described space qualified optical attenuators.
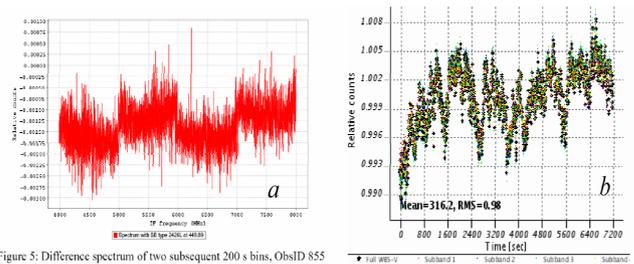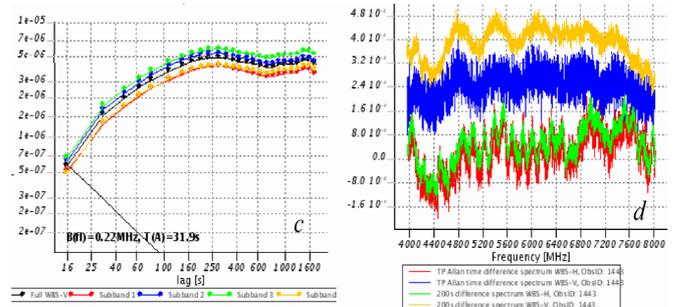

Fig. 6. Things that can go wrong. a) platforming, b) gain instability due to the LO in this case, c) very short Allan times, significant baseline distortion.

V LO WARM UP TIME

Local oscillator warm up time has a direct bearing on the planned AOT's. During ILT the local oscillator units were not preheated. This is planned for flight, and it is possible that the stabilization can be shortened a bit.

We provide here the 5τ warm-up times for Total Power (continuum) and differential stabilization. In general, the higher frequency multipliers are more complex and need a longer (50 min) warm-up time then the lower frequency multipliers (30 min).

TABLE I. HIFI LO WARM UP TIMES.

Band	Total Power (min)	Frequency (GHz)	Obsid	Differential (min)	Frequency (GHz)	Obsid
1a	30	509	268476280	5	494	268510476
1b	30	582	268461236	3.5	563	268510729
2a	40	640	268459469	10	640	268511312
2b	40	736	268461220	13	728	268511362
3a	40	812	268471048	20	814	268511420
3b	40	878	268471066	13.5	869	268511669
4a	30	995	268483530	15	982	268509805
4b	40	1095	268460379	20	1108	268510072
5a	30	1185	268459366	10	1127	268510773
5b	40	1180	268460362	10	1191	268510564
6a	50	1462	268467526	15	1444	268511851
6b	47	1599	268471030	15	1581.4	268512252
7a	50	1723	268471084	7 ?	1716.6	268513243
7b	55	1897	268471102	x	x	x

SIS bands
HEB bands. Frequent LO tuning needed during first 2-3τ (Total Power time period).

For certain differential observations one may not be too interested in the LO drift, provided that the change in LO pump level is not so large that the mixer unit operation is completely out of specification. This is not merely an academic exercise, it has in fact been observed in the HEB mixer bands that the LO pump level can drift out of the operating regime of the mixer.

To circumvent these problems, it is now planned to automatically retune all local oscillator ~ 5 minutes after switch on, and do a second retune of the HEB local oscillators after an additional 500 s. For differential observation such as DBS and LS typically a 10 minute wait period is sufficient. Of course this does require careful planning of the observation.

VI EFFECT OF USING A DIPLEXER

We show in Fig. 7 the stability and sensitivity statistics of SIS mixer band 1b, as measured on the wide band spectrometer (4-8 GHz). In case of a *beam splitter* band (HIFI band 1, 2, 5) we consistently find the following: The system temperatures (no atmosphere) are reasonably constant across the 4-8 GHz IF passband. However, the spectroscopic Allan times, though uniform for WBS subband 1-3 (4-7 GHz), and generally a bit depressed in subband 4 (7-8 GHz).
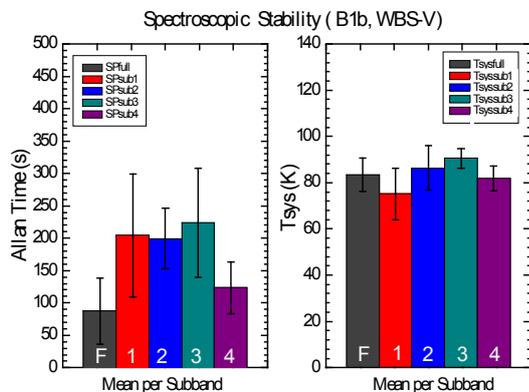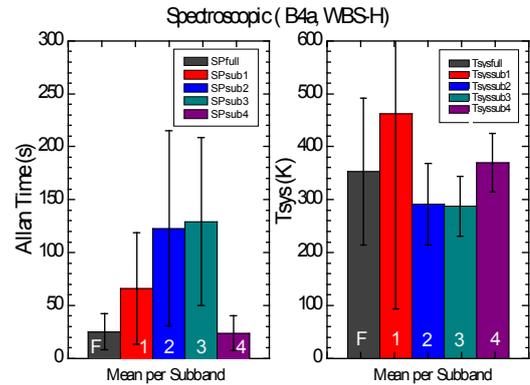

Fig. 8. Band 4a Spectroscopic Allan variance and system noise temperature statistics. Band 4a is a 'diplexer' LO injection band. Subbands 2, 3 (5-7 GHz) are generally the most stable, followed by subband 1 and 4.

The spectroscopic stability averaged over the entire spectrometer band is always less than that of the individual subbands.

For the *SIS diplexer* bands 3 & 4 we find that the two centre subbands are the most sensitive and stable (5-7 GHz), and that the stability and sensitivity of subband 1, 4 is somewhat degraded. WBS subband 1 is generally a bit more sensitive and stable then subband 4. This of course reflects the diplexer passband profile. Instability can be attributed to optical reflections in the front end. This is shown in Fig. 8 for mixer band 4a.

At this point it should be noted that during the ILT, the FPU (4 K) and LOU (~120 K) were cryogenically cooled by means of a hybrid cryostat (compressor and LHe). This resulted in a ± ~10 μm mechanical modulation of the LO-mixer standing wave. In flight, with an all LHe cryostat, this situation is hopefully much more stable, and it is not unreasonable to expect a better stability performance of WBS subband 1. The one caveat is that the reaction wheels of the spacecraft will introduce 'high frequency' vibrations.

Fig. 7. Band 1b Spectroscopic Allan variance and system temperature statistics. Band 1b is a 'beamsplitter' LO injection band. Sensitivity is uniform, but the stability is generally worst in WBS subband 4.
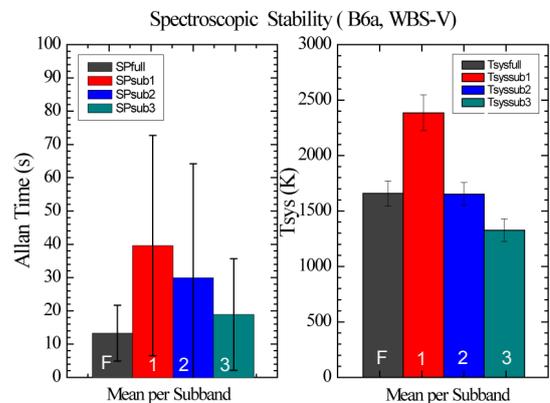

Fig. 9. Band 6a Spectroscopic Allan variance and system temperature statistics. Band 6a is a 'diplexer' LO injection band. Subband 3 (2.4-3.4 GHz) is the most sensitive, but also the most spectroscopically unstable.

For the *HEB mixer diplexer* bands, subband 3 is always the most sensitive being the lowest in IF frequency (2.4-3.4 GHz), but also the most unstable (Fig. 9). This is caused by the roll-off in mixer conversion gain of the HEB mixer (due to the finite electron and phonon relaxation time [13]) starting at approximately 3 GHz. Thus WBS subband 1 is the most stable, but also the least sensitive. Narrow spectral line observations should therefore be planned in the lower part of the HEB B6 and B7 IF band.

VII PARAMETRIC STUDIES

As part of the HIFI instrument level test program (ILT), parametric studies of the HEB mixer band 6 & 7 were performed. In addition, we have also looked at the effect of small deviations in magnetic field setting for the SIS bands.

For the HEB mixer bands. two situation were examined: System stability as a function of LO power (HEB current), and system stability as a function of HEB bias voltage. In Fig. 10 we show the normalized spectroscopic Allan variance as a function of LO power. For the HEB bands 30 μA is slightly over pumped, 40 μA optimally pumped, and 50 μA on the verge of being under pumped. Slightly over pumping the HEB mixer from a stability point of view appears beneficial. This is understood to be the combined effect of a small decrease in sensitivity and an increase in required LO pump level. Higher LO power levels generally causes the W-band power amplifiers in the LO chain to run more saturated, thereby clipping the amplitude modulated (AM) noise on the LO carrier signal [14]. Consistent also is the trend that lower LO power (HEB current) results in a reduced Allan time, around 10 s in our case. This agrees with the picture that AM noise is present on the LO carrier, and that saturation of the LO chain power amplifiers is extremely important. In Fig.11 we show the normalized spectroscopic Allan variance as a function of bias voltage for a nominal LO pump level. Again we have a consistent trend, higher HEB bias voltages provide more stable mixer behavior.
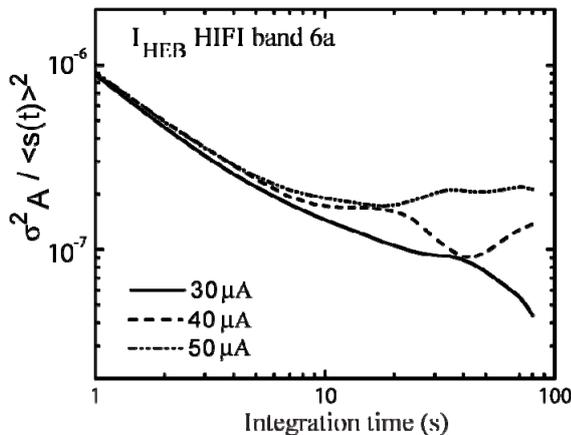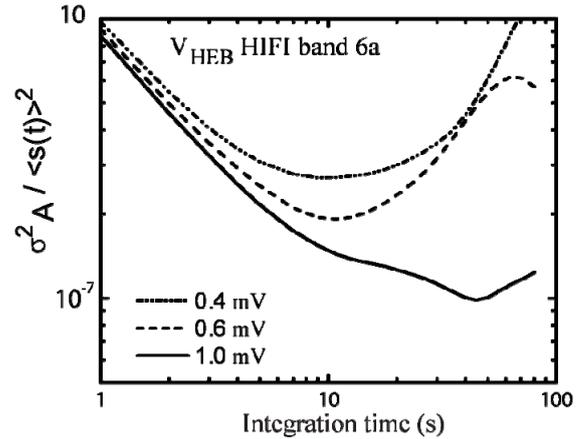

Fig. 11 Band 6a, normalized spectroscopic stability as a function of HEB mixer bias voltage. Optimal sensitivity is typically achieved around 0.5~mV. vLO=1666 GHz

At the larger (1 mV) bias voltage this is simply related to the sensitivity of the HEB mixer, e.g. the less sensitive the mixer the less sensitive it will also be to AM local oscillator noise. However between 0.4 and 0.6 mV the sensitivity of the mixer is more or less constant and the instability is more likely the result of how close the mixer is biased to the (known) HEB mixer instability region [12, 15]. From this discussion it is clear that slightly over pumping the HEB mixer (20 %), while biasing it above the nominal operating voltage (20 %) enhances the mixer stability, and thereby integration efficiency and baseline quality.

VIII INSTRUMENT STABILITY AND BASELINE QUALITY

Throughout the thesis instrument stability is discussed as an important system parameter in establishing time efficient observations. Considering the generally large expense, demand on telescope time, and quality of data, stability has become an important design parameter for modern heterodyne instrumentation.

Fig. 10 Band 6a, normalized spectroscopic stability as a function of LO pump level. HEB mixer band 6a. 30 μA is slightly over pumped, 40 μA optimally pumped, and 50 μA on the verge of being under pumped. The LO frequency is 1666 GHz.
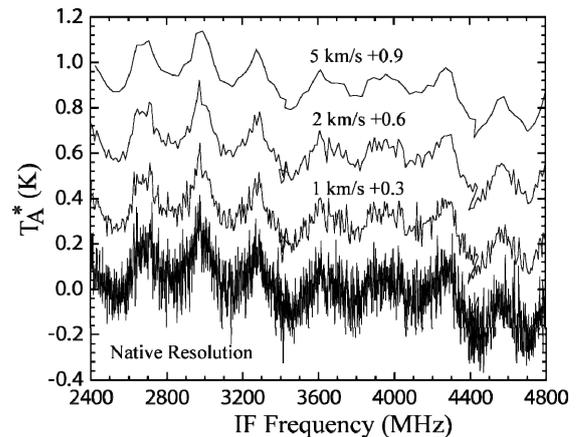

Fig. 12 Synthesized position switched spectrum for HEB mixer band 7b. Total 'on-source' integration time in one 600 s cycle is ~464 s, clearly much too long given the stability of the mixer. Severe baseline distortion is the result. vLO=1.890 THz, V-polarization sensitive mixer.
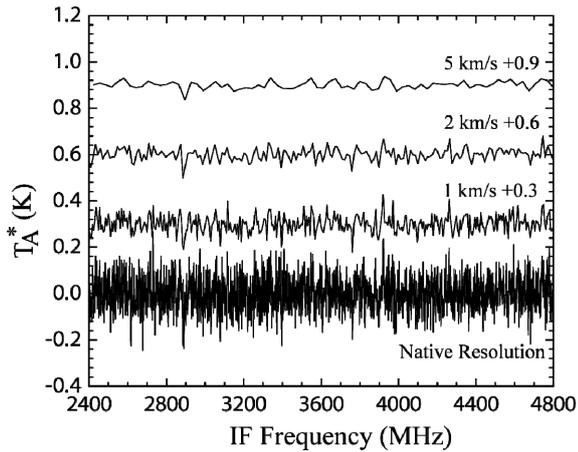
Fig. 13. Synthesized double beam switched (DBS) spectrum for different velocity resolutions. Each phase of the chop cycle is 4 s, well below the stability time of the instrument. For a native resolution, the theoretical and synthesized 1σ rms noise levels are virtually identical (64~mK vs. 68 mK). Total 'on-source' integration time is 2829 s. $\nu_{LO}=1.890$ THz, V-polarization sensitive mixer.

In Fig.'s 12, 13 we depict a simulated position- and DBS spectra from actual HIFI [4] data, as obtained in HEB mixer band 7 during instrument level tests (ILT). The spectra are shown for four different velocity binning resolutions; native (0.086 km/s), 1km/s, 2km/s, and 5km/s. To convert the velocity resolution to spectral resolution we use the Doppler relationship $v=c/R$ where $R=v/\Delta v$. The corresponding spectral resolution Δv may thus be obtained as: native 0.5462 MHz [1], 6.33 MHz, 12.67 MHz, and 31.67 MHz. The associated total power and spectroscopic Allan variance is depicted in Fig's 14, 15.

For standard position switch observations the source is observed for a time t_{on}, after which an off-source t_{off} reference measurement is taken. The duration of the reference measurement is ordinarily $\sqrt{t_{on}}$. To remove the sky, telescope and instrumental baselines, the 'on' source signal is subtracted from the 'off' source signal as part of the calibration routine. For a 'stable' receiver (instrument) position switching is the
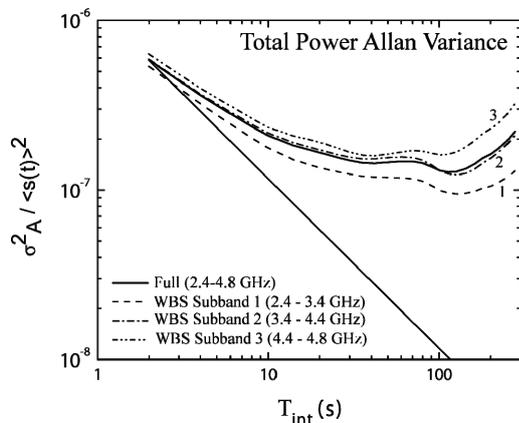

Fig. 14. Total power stability of HIFI HEB mixer band 7 at 1.8970 THz. The Allan time, in a fluctuation noise bandwidth of ~1.8 MHz, is ≤ 8 s.
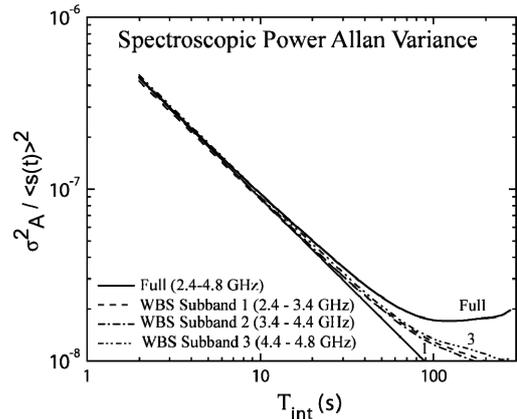

Fig. 15. Spectroscopic stability (text) with a measured stability time of ~80 s.

most efficient method of observing, since a relatively large percentage of the time is spend integrating on the source. Unfortunately for HEB based heterodyne receivers, 'stable' appears to be a bit of an oxymoron, as evidenced by the total power Allan variance stability measurement of Fig. 14. Typical total power Allan variance times, defined by a $\ge \sqrt{2}$ deviation from the ideal radiometer response, are commonly less than 8 s. The spectroscopic stability may be as large as ~80 s in a 1.8~MHz noise fluctuation bandwidth (Δv). In Fig. 12 we show a synthesized position switched spectrum with an 'on-source, slew time, off-source, and again slew time' cycle of 600 s. Total on-source integration time of the entire data set is 2789 s. For the Herschel space observatory the roundtrip slew time is assumed 80 s. In position switch mode, each 600 s cycle thus spends ~ 464 s integrating on the source with the remainder in slew time (80 s) and off-source integration (~56 s). Clearly the 'on-off' switching time is much larger than the spectroscopic stability time of the system. This is evidenced by the extremely poor baseline quality of Fig. 12.

A far better, though less efficient approach, is to symmetrically beam switch at a rate less then the spectroscopic Allan stability time of the system, for example by means of nutating mirror. In Fig. 13 we show the result of a double-beam switch (DBS) 0.25~Hz 'off-on-on-off' slow-chop pattern. Again each cycle is 600 s and includes one position switch cycle as described above. Including the telescope chopping efficiency and position switch overhead, the total integration time is 2829 s.

To estimate T_A^* and compare it to the 1σ noise obtained from the SSB spectrum of Fig. 14, we use Eq. 1 with $\Delta v = 1.8$ MHz. Note that this is larger then the intrinsic spectral resolution of the spectrometer (1 GHz/2000 channels).

Given a measured DSB HEB receiver noise temperature (in the lower region of the IF band) of ~ 1600 K, we calculate a theoretical 1σ rms noise level of 64 mK. This compares favorably with the, from the spectrum of Fig. 14 obtained 1σ rms noise level of 68 mK (native resolution). Thus we find that symmetric beam switching on time scales less then the spectroscopic Allan time provides proper baseline quality with rms noise levels in agreement with theory. The penalty.
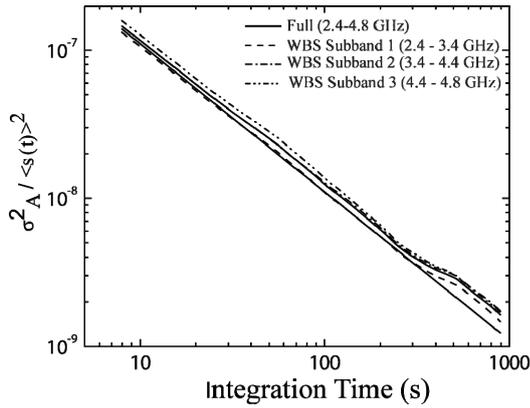
Fig. 16. Measurement of the internal load differential stability on HEB mixer band 7b (1.890 THz, C[+]).

of differential beam switch measurements over (ideal) position switch measurements is a factor 2 increase in the rms noise level. The overwhelming benefit is of course the quality of the obtained baseline (spectra). The popular use of DBS techniques (analogous to synchronous detection) comes therefore as no surprise.

In Fig. 16 we shown an example of a Band 7b differential internal load measurement. This information is useful in determining how often secondary loop calibrations need to be taken. In case of the HEB mixers it appears that 900 s (15 min) is adequate

IX RESULTS

The HIFI system stability was measured at a large number of proposed line frequencies, for all 14 LO subbands. A list is compiled in Table II. It is indicative of the HIFI instrument potential, e.g. continuous coverage from 480 GHz – 2 THz.

Table II. List of frequencies at which the HIFI instrument ILT stability data was taken. The table lists all 14 LO subbands. The frequencies were carefully chosen at astronomically relevant lines (Upper or Lower sideband). In essence, HIFI may be thought of as 14 different heterodyne receivers with associated local oscillator units.

B1a (488-552)				B1b (556-628)		
Line	νlo (GHz)[1,2,5]	νline (GHz)	Proposal	Line	νlo (GHz)[1,2]	νline (GHz)	Proposal
O2	494	487.2	key	H2O-ortho	563	556.936	19
H2O	494	488.49	3	HDO	566	559.816	1
C	498	492.161	3	NHh3-ortho	566	572.498	7
HDO	516	509.329	3	HDO	593	599.927	2
ND	526	522.077	4	D2O	614	607.35	3
CH	527	532.721	3	H2O-ortho	618	620.701	4
CH	531	536.761	6	HCO+	618	624.205	1
H2[18]O-ortho	542	547.676	18	H2O+	625	631.773	4
H2[17]O-ortho	548	552.021	5				

B2a (642-710)				B2b (724-793)		
Line	νlo (GHz)[1,2,5]	νline (GHz)	Proposal	Line	νlo (GHz)[1,2]	νline (GHz)	Proposal
H2O-para	640	645.834	2	CS	728	734.32	2
H2O18		647.198		H2[18]O-ortho		745.32	
	652.5		2		739.5		3
H2O-ortho	652.5	658.007	3	H2O-ortho	744	750.572	2
H2O18	667	661.356	2	H2O-para	758	752.033	14
D2H+	686	691.66	6	[13]CO	765	771.184	2
H2O18	698	692.079	2	HDO	772	766.166	1
SiO	700	694.275	2	O2	779	773.8	5
O2	709	715.4	0	x	788	784	x

B3a (807-852)				B3b (866-953)		
Line	νlo (GHz)[1,2,5]	νline (GHz)	Proposal	Line	νlo (GHz)[1,2]	νline (GHz)	Proposal
CO	812	806.652	0	H2O-ortho	869	863.855	0
C	814	809.342	3	[13]CO	878	881.273	0
13CH+	823	830.131	5	HDO	887	893.639	7
O2	827	834.1	?	D2O	902	897.947	3
CH+	837	835.071	11	H2O	912	906.206	0
H2CO	849	855.151	0	H2O-para	922	916.171	2
H2O-para	852	859.859	0	COh	928	921.8	6
				CH2	x	945.8	6
				NHh2	946.5	952.542	6

B4a (957-1053)				B4b (1054-1114)		
Line	νlo (GHz)[1,2,5]	νline (GHz)	Proposal	Line	νlo (GHz)[1,2]	νline (GHz)	Proposal
NH	968	974.462	13	HCN	1068	1062.983	0
H2O-ortho	974	968.048	3	H2S	1080	1072.8	0
OH+	977.8	971.804	9	H2O18	1089.6	1095.627	6
NH	981.2	974.462	13	H2O-ortho	1091.3	1097.364	12
H3O+	990.6	984.6	10	C[13]Oh	1095	1101.35	10
H2O-para	995	987.927	18	H2[18]O-para	1107	1101.698	18
H2[18]O-para	1000.6	994.675	6	H2O-para	1108	1113.343	20
NH+	1006.5	1012.524	5	H2O+	1110	1115.086	7
CO	1031	1036.912	2				

B5a (1127-1178)				B5b (1192-1242)		
Line	νlo (GHz)[1,2,5]	νline (GHz)	Proposal	Line	νlo (GHz)[1,2]	νline (GHz)	Proposal
O2	1127	1120.715	3	H2CO	1180	1185	0
H2O+	1145.5	1139.515	2	H2O-para	1191	1196.859	6
CO	1145.5	1151.985	13	H2O-para	1202	1207.666	6
H2O-ortho	1159	1153.118	9	NH3	1209	1214.859	4
H2O-ortho	1164	1158.324	3	HDO	1223	1217.3	10
H2O-ortho	1168	1162.931	3	H2O-para	1223	1228.799	18
H2O-para	1168	1172.448	0	H2O-para	1235	1228.799	18
H2[18]O-ortho	1187	1181.394	0	HF	1238	1232.476	7
H2O-para	1202	1207.666	6				

Line	νlo (GHz)[1,2,5]	νline (GHz)	Proposal				
				x	1581.4	1585	0
H2O	1444	1440.782	0	CO	1608	1611.793	0
HCl+	1447	1444	0	H2[18]CH	1630	1633.484	0
N II	1457.5	1461.134	4	13CH	1643.6	1647.239	4
D2H+	1480.2	1476.6	3	H2O+	1653	1655.813	9
CH	1480.2	1477.292	0	CH	1652.8	1656.961	8
CO	1493.3	1496.923	3	H2O-ortho	1665.2	1661.011	5
H		1532.6		H2[17]O-ortho		1662.464	
	1529		0		1665.2		3
13CO	1544.5	1540.988	0	H2O-ortho	1667.4	1669.905	21
	1548	1551.6	0	x	1686	1689	2
				x	1692	1689	2

B7a (1700-1800)				B7b (1720-1905)		
Line	νlo (GHz)[1,2,5]	νline (GHz)	Proposal	Line	νlo (GHz)[1,2]	νline (GHz)	Proposal
H2O-ortho	1716.5	1713.94	1	CO	1728	1726.602	3
H2[18]O	1723	1719.25	0	H2O-para	1801	1797.238	1
H2O-ortho	1720.3	1716.765	8	OH	1834	1837.747	7
CO	1730.2	1726.602	3	CO	1845	1841.346	9
H2O-ortho	1757.2	1753.888	3	H2O-ortho	1872	1867.825	6
13CO	1757.2	1760.486	3	HCl	1872	1876.23	3
H2O-para	1762.5	1766.121	0	CH4	1885.6	1882	3
HCN	1773.5	1769.876	0	[13]C+	1897	1900.545	21
H2O-ortho	1794	1797.238	0	CH2	1904.1	1907.987	3

Tables III – VI list the system and differential stability of the instrument. The first number is the mean, the second value the standard deviation (scatter). Due to space the high resolution spectrometer (HRS) results are not shown here. They amount however to very similar numbers.

Table III. WBS-V Total Power for all 14 mixer Sub-bands.

band	Freq. (GHz)	Continuum[1-4] Stability (mean/std) spec > 5s		Spectroscopic[1-4] Stability (mean/std) spec > 75s	
		Full	Best SubBand	Full	Best SubBand
B1a	488-522	22.4/9.7	35.0/14.2	89.0/41.4	303.9/102.4
B1b	566-628	25.7/12.9	29.7/16.5	87.9/51.1	223.4/84.2
B2a	642-710	17.7/11.8	23.9/11.8	94.5/26.8	324.0/129.8
B2b	724-793	12.7/6.7	15.2/7.4	86.1/41.2	246.1/91.9
B3a	807-852	6.4/3.8	6.8/3.8	21.5/11.4	99.8/53.2
B3b	866-953	13.1/7.5	13.9/8.0	56.1/27.4	192.6/85.0
B4a	980-1040	9.0/4.5	10.6/7.0	37.7/24.9	178.4/109.2
B4b	1065-1115	15.4/3.3	20.8/4.6	46.8/12.3	150.3/52.3
B5a	1127-1178	19.2/5.6	31.1/6.4	105.2/31.6	280.3/105.3
B5b	1192-1242	19.1/5.2	27.4/7.1	83.4/33.3	190.1/56.4
B6a	1430-1570	5.1/3.1	5.4/2.8	13.3/8.4	39.6/33.1
B6b	1580-1690	4.5/2.1	4.9/2.0	20.2/11.0	59.4/30.0
B7a	1692-1845	7.8/6.9	8.2/6.9	21.7/12.7	54.0/23.2
B7b	1719-1908	6.0/4.9	6.0/4.9	13.2/16.1	25.3/31.1

Table IV. WBS-H Total Power for all 14 mixer Sub-bands.

band	Freq. (GHz)	Continuum[1-4] Stability (mean/std) spec > 5s Full	Best SubBand	Spectroscopic[1-4] Stability (mean/std) spec > 75s Full	Best SubBand
B1a	488-522	17.2/5.0	27.6/11.3	72.8/17.1	210.9/94.9
B1b	566-628	17.0/7.8	21.0/7.2	65.8/24.9	161.6/70.9
B2a	642-710	17.7/4.5	26.9/7.1	68.4/14.1	286.8/129.6
B2b	724-793	12.0/5.8	16.2/8.3	77.8/21.7	243.7/123.4
B3a	807-852	9.1/3.8	9.6/4.7	33.8/19.7	93.4/71.8
B3b	866-953	9.9/3.4	11.5/4.0	68.8/39.8	130.6/67.2
B4a	980-1040	8.0/3.8	10.6/4.9	25.1/17.0	129.3/79.6
B4b	1065-1115	12.4/3.3	14.9/7.3	45.0/15.8	152.7/56.8
B5a	1127-1178	15.6/5.8	26.0/8.3	79.5/17.9	240.2/64.4
B5b	1192-1242	18.7/6.5	27.4/6.0	76.0/13.7	174.6/45.5
B6a	1430-1570	3.8/2.5	4.9/2.8	10.0/5.2	32.8/30.8
B6b	1580-1690	4.8/3.1	5.8/2.8	19.8/8.2	54.8/20.2
B7a	1692-1845	4.0/2.3	4.7/2.1	15.3/6.7	51.1/14.0
B7b	1719-1908	4.2/2.9	4.2/2.9	9.1/11.0	21.4/25.1

Table V. Differential stability WBS-V.

band	Freq. (GHz)	Diff. Load-Chop[1-4] Spectroscopic spec > 600s Full	Best SubBand	Diff. Internal-Load[1-4] Spectroscopic spec > 600s Full	Best SubBand	Diff. Load-Switch (DBS)[1] Spectroscopic spec > 600s Full	Best SubBand
B1a	488-522	> 1800	> 1800	359.4	>=650	>> 2250	>> 2250
B1b	566-628	> 1800	> 1800	279.5	>=650	>> 2250	>> 2250
B2a	642-710	> 1800	> 1800	>=700	>=650	>> 2250	>> 2250
B2b	724-793	> 1800	> 1800	558.9	718.6	>> 2250	>> 2250
B3a	807-852	>> 900	>> 900	103.7	574.2	> 1800	> 1800
B3b	866-953	>> 900	>> 900	>=650	>=650	> 1800	> 1800
B4a	980-1040	>> 900	>> 900	451.8	>=850	>> 2250	>> 2250
B4b	1065-1115	>> 900	>> 900	800.6	>=850	> 2250	> 2250
B5a	1127-1178	>> 900	>> 900	>=850	>=850	> 1800	> 1800
B5b	1192-1242	>> 900	>> 900	>=850	>=850	> 1800	> 1800
B6a	1430-1570	>> 900	>> 900	700	>=800	> 1800	> 1800
B6b	1580-1690	>> 900	>> 900	642	>=800	> 1800	> 1800
B7a	1692-1845	>> 900	>> 900	700	>=800	> 1800	> 1800
B7b	1719-1908	>> 900	>> 900	700	>=800	> 1800	> 1800

Table VI. Differential Stability WBS-H. Internal Load is important for the calibration loop (Fig. 16).

band	Freq. (GHz)	Diff. Load-Chop[1-4] Spectroscopic spec > 600s Full	Best SubBand	Diff. Internal-Load[1-4] Spectroscopic spec > 600s Full	Best SubBand	Diff. Load-Switch (DBS)[1] Spectroscopic spec > 600s Full	Best SubBand
B1a	488-522	> 1800	> 1800	575	>=650	>> 2250	>> 2250
B1b	566-628	> 1800	> 1800	279.5	>=650	>> 2250	>> 2250
B2a	642-710	> 1800	> 1800	717.7	>=850	>> 2250	>> 2250
B2b	724-793	> 1800	> 1800	718.6	814.4	>> 2250	>> 2250
B3a	807-852	>> 900	>> 900	250	300	> 1800	> 1800
B3b	866-953	>> 900	>> 900	>=650	>=850	> 1800	> 1800
B4a	980-1040	>> 900	>> 900	190.2	>=850	>> 2250	>> 2250
B4b	1065-1115	>> 900	>> 900	850	>=850	1870	> 2250
B5a	1127-1178	>> 900	>> 900	>=850	>=850	> 1800	> 1800
B5b	1192-1242	>> 900	>> 900	>=850	>=850	> 1800	> 1800
B6a	1430-1570	>> 900	>> 900	604.5	>=800	> 1800	> 1800
B6b	1580-1690	>> 900	>> 900	700	>=800	> 1800	> 1800
B7a	1692-1845	>> 900	>> 900	700	>=800	> 1800	> 1800
B7b	1719-1908	>> 900	>> 900	700	>=800	> 1800	> 1800

Table VII. Expected System temperatures (no atmosphere) with DBS (on-off) source observations for each subband. On source integration time is 5 minutes.

band	Freq. (GHz)	WBS-V Tsys SSB (K) Mean	WBS-V RMS (mK) in 600s Mode=Diff	WBS-H Tsys SSB (K) Mean	WBS-H RMS (mK) in 600s Mode=Diff
B1a	488-522	144.2	8.3	150	8.7
B1b	566-628	166.8	9.6	180	10.4
B2a	642-710	275.8	15.9	246	14.2
B2b	724-793	325.2	18.8	398	23.0
B3a	807-852	631.6	36.5	209.7	12.1
B3b	866-953	538.6	31.1	934.2	53.9
B4a	980-1040	805.4	46.5	706	40.8
B4b	1065-1115	807	46.6	717.6	41.4
B5a	1127-1178	1918.8	110.8	1588.2	91.7
B5b	1192-1242	2658.8	153.5	2070.2	119.5
B6a	1430-1570	3317.8	191.6	3004.8	173.5
B6b	1580-1690	3133.2	180.9	2855.2	164.8
B7a	1692-1845	3394.8	196.0	2808.4	162.1
B7b	1719-1908	3705.8	214.0	3185.4	183.9

X CONCLUSION

We have measured the IF stability, system stability and differential gain stability of the HIFI instrument, to be flown on board the Herschel space satellite. Warm-up time constants for the IF and LO have been established and will be used in the AOT's. Parametric studies have been performed to access the impact of mistuning. This is especially relevant for HIFI since up/down link telemetry is only once a day.

From the measured data we have determined the loss in integration efficiency for each LO subband (14). We have also examined the instrument for platforming, baseband ripple and optimum observing strategy.

Finally, the information is being fed to the Herschel observation planing too (HSPOT)[16]. This will help make realistic time estimates of the requested astronomical sources.

New observation modes have been defined as an outcome of the ILT: OTF and raster scans with load-chop. Though not the most efficient mode of operation, they will provide the high quality data anticipated.

The next phase is to prepare for the thermal vacuum and performance verification in flight.

XI ACKNOWLEDGMENT

To obtain a measure of the achievable sensitivity levels of the instrument, we list in table VII the expected 1σ noise level in a 10 minutes Observation (Eq. 1). Because the instrument is sensitive to both H and V polarizations the actual rms noise will be √2 lower then indicted in Table VII, e.g.

$$T_A^* = \frac{\sqrt{2} T_{sys}^{SSB}}{\sqrt{\eta_c \Delta \nu T}} \ .$$

(8)

T_A^* is the on source antenna temperature (K).

REFERENCES

[1] R.Schieder, O. Siebertz, F. Schloeder, C. Gal, J. Stutzki, P. Hartogh, V. Natale, "Wide-Band Spectrometer for HIFI-FIRST" Proc. of ``UV, Optical, and IR Space Telescopes and Instruments, J. B. Breckinridge, P. Jakobsen Eds., SPIE 4013, 313-324, Jul., (2000).

[2] O. Siebertz, "Akusto-optisches Spektrometer mit variabler Auflsung", PhD thesis, University Cologne, (1998).

[3] M. Belgacem, L. Ravera, E. Caux, P. Caïs & A. Cros: "The high resolution versatile digital spectrometer of HIFI-HSO", New Astronomy 9, 43, 2003.

[4] Th. de Graauw, N. Whyborn, E. Caux, T. G. Phillips, J. Stutzki, X Tielens, R. G\"usten, F. P. Helmich, W. Luinge, J. Pearson, P. Roelfsema, R, Schieder, K. Wildeman, and K. Wavelbakker, "The Herschel-Heterodyne Instrument for the Far-Infrared (HIFI)" [Online]. Available: herschel.esac.esa.int/Publ/2006/SPIE2006_HIFI_paper.pdf

[5] [Online]. Available: Herschel; http://sci.esa.int/

[6] J. W. Kooi, J. J. A. Baselmans, A. Baryshev, R. Schieder, M. Hajenius, J. R. Gao, T. M. Klapwijk, B. Voronov, and G. Gol'tsman, "Stability of Heterodyne Terahertz Receivers", Journal of Applied Physics, Vol. 100, 064904, Sep. (2006).

[7] R. Schieder, "Characterization and Measurement of System Stability", SPIE, Vol. 598, Instrumentation for Submillimeter Spectroscopy (1985).

[8] R. Schieder, C. Kramer, "Optimization of Heterodyne Observations using Allan variance Measurements", Astron. Astrophys, Vol. 373, 746-756 (2001).

[9] J.W. Kooi, G. Chattopadhyay, M. Thielman, T.G. Phillips, and R. Schieder, "Noise Stability of SIS Receivers", Int. J. IR and MM Waves}, Vol. 21, No. 5, May, (2000).

[10] V. Ossenkopf, "The stability of spectroscopic instruments: a unified Allan variance computation scheme", A & A, Vol. 479, 915-926 (2008).

[11] D. W. Allan, "Statistics of Atomic Frequency Standards", Proc. IEEE, Vol. 54, No. 2, pp 221-230, (1969).

[12] A. Cherednichenko, V. Drakinskiy, T. berg, P. Khosropanah, and E. Kollberg, "Hot-electron bolometer terahertz mixers for the Herschel Space Observatory", Rev. Sci. Instrum., Vol. 79, 034501(2008).

[13] J. W. Kooi, J. J. A. Baselmans, J. R. Gao, T. M. Klapwijk, M. Hajenius, P. Dieleman, A. Baryshev, "IF Impedance and Mixer Gain of NbN Hot-Electron Bolometers", Journal of Applied Physics, Vol. 101, 044511, Feb. (2007)

[14] N. Erickson, "AM Noise in Drives for Frequency Multiplied Local Oscilators", Proc 15ᵗʰ Int. Symp. on Space Terahertz technology Northampton, MA, (2004), pp. 135-142.

[15] M. Hajenius, J. J. A. Baselmans, A. Baryshev, J. R. Gao, T. M. Klapwijk, J. W. Kooi, W. Jellema, and Z. Q. Yang, "Full characterization and analyses of a THz heterodyne receiver based on a NbN hot electron bolometer", J. Appl. Phys., Vol. 100, 074507 (2006).

[16] [Online]. Available: http://herschel.esac.esa.int/ao_kp_tools.shtml/